Catena 202 (2021) 105255

Contents lists available at ScienceDirect

Catena

journal homepage: www.elsevier.com/locate/catena

Clay-plug sediment as the locus of arsenic pollution in Holocene alluvial-plain aquifers

S. Kumar [a], D. Ghosh [b], M.E. Donselaar [a,c,*], F. Burgers [a], A.K. Ghosh [d]

[a] Department of Applied Geoscience and Engineering, Delft University of Technology, P.O. Box 5048, 2600 GA Delft, the Netherlands
[b] Laboratory of Biogeochem-mystery, Centre for Earth Sciences, Indian Institute of Science, C.V. Raman Avenue, Bengaluru, Karnataka 560012, India
[c] Department of Earth and Environmental Sciences, Division of Geology, KU Leuven, Celestijnenlaan 200E, B-3001 Leuven, Belgium
[d] Mahavir Cancer Sansthan and Research Centre, 4th Floor Phulwari Sharif, Patna 801505, India

ARTICLE INFO

Keywords:
Abandoned meandering-river bends
Point-bar geomorphology
Permeability anisotropy
Satellite-image analysis
Total arsenic load

ABSTRACT

Shallow aquifers in many Holocene alluvial basins around the world have in the last three decades been identified as arsenic pollution hotspots, in which the spatial variation of natural (or: *geogenic*) arsenic concentration is conditioned by the meandering-river geomorphology and the fluvial lithofacies distribution. Despite the large amount of publications on the specifics of the pollution, still many uncertainties remain as to the provenance and processes that lead to arsenic enrichment in aquifers. In this paper, arsenic in abandoned and sediment-filled meandering-river bends (or: *clay-plugs*) is highlighted as a primary source of aquifer pollution. The combination of high organic-carbon deposition rates and the presence of chemically-bound natural arsenic in sediment of this specific geomorphological setting creates the potential for microbially-steered reductive dissolution of arsenic in an anoxic environment, and subsequent migration of the desorbed arsenic to, and stratigraphic entrapment in, adjacent sandy point-bar aquifers. To assess the magnitude of the arsenic source in clay-plug, bulk sediment volume calculations were made of twenty clay plugs on the Middle Ganges Plain of Bihar (India), by combining clay-plug surface area analysis of Sentinel-2 satellite data, side-scan sonar depth profiling of oxbow lakes and the Ganges River, and sedimentological data from five cored shallow wells. ICP-MS based elemental analysis of 36 core sub-samples, complemented with published concentration data in a similar geomorphological setting in West Bengal, India, yielded an average arsenic content of 28.75 mg/kg sediment in the 12-m-thick clay plugs, which amounts to a total arsenic volume of $0.07 - 3.13 \cdot 10^6$ kg per clay plug. A scenario is presented for the release of arsenic from the clay-plug sediment by microbial metabolism, followed by migration of the desorbed arsenic to the bordering point-bar sands.

1. Introduction

Arsenic-bearing aquifers pose a worldwide, severe health hazard for many millions of people who lack access to controlled piped water systems for consumption and irrigation (Smith et al., 2000). Long-term exposure to arsenic-polluted water with concentrations far above the recommended permissible limit of 10 μg/L (WHO, 1993, 2011), by direct ingestion and via arsenic-contaminated food consumption (Mondal et al., 2021), results in the accumulation of arsenic in the human body and a wide array of diseases generally grouped as arsenicosis (Saha, 2003; Chikkanna et al., 2019). The arsenic pollution is specifically severe in shallow (to approximately 40 m depth) aquifers in the Ganges-Brahmaputra-Meghna Delta in West Bengal, India and Bangladesh (Saha, 1984, 2009; Guha Mazumder et al., 1988; Das et al., 1994; Bhattacharya et al., 1997, 2002; Acharyya et al., 2000; BGS and DPHE, 2001; Smedley and Kinniburgh, 2002; Ahmed et al., 2004; Zheng et al., 2005; Von Brömssen et al., 2007, 2008; Shah, 2008, 2010, 2017; Ravenscroft et al., 2009; Mukherjee et al., 2011). In terms of geomorphological setting, many of the polluted aquifers occur in Holocene meandering-river landscapes (Zheng et al., 2005; Shah, 2008; Weinman et al., 2008; Sahu and Saha, 2015; Donselaar et al., 2017). Common denominator is the large spatial variation in concentrations of naturally occurring (or: *geogenic*) arsenic in the groundwater, which is controlled by the geomorphology of the river landscape and by the spatial distribution of sedimentary facies and inherent porosity and permeability anisotropy (Weinman et al., 2008; Donselaar et al., 2017; Jakobsen

* Corresponding author.
E-mail address: m.e.donselaar@tudelft.nl (M.E. Donselaar).

https://doi.org/10.1016/j.catena.2021.105255
Received 5 September 2020; Received in revised form 6 January 2021; Accepted 14 February 2021
Available online 16 March 2021

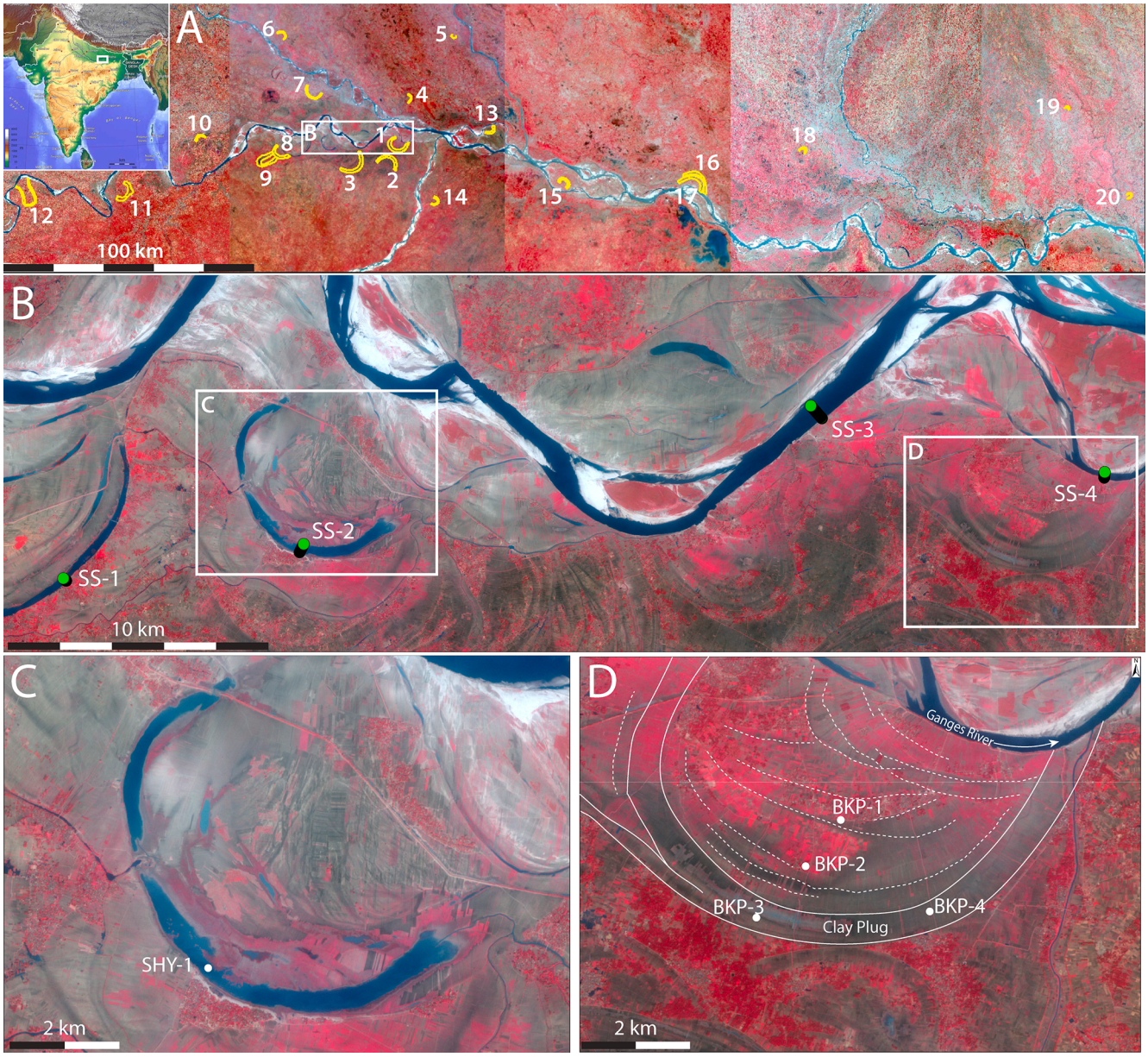

Fig. 1. Sentinel-2 satellite images (Nov. 2017) with 10 m spatial resolution and NIR, Red, Green and Blue bands. Dark red: trees and plants; pink/light: vegetation/crops; grey: wetland or barren land. A. Location of the twenty clay plugs from which surface areas have been calculated. B: Location map of side-scan sonar profiles SS-1 to SS-4. C: Suhiya oxbow lake with location of well SHY-1. D: Bakhorapur clay plug and point bar with well locations BKP-1 to BKP-4. Clay plug outlined with solid white lines. Dashed lines: ridge-and-swale morphology on the point bar. (For interpretation of the references to colour in this figure legend, the reader is referred to the web version of this article.)

et al., 2018). In addition to the Ganges-Brahmaputra-Meghna Delta, examples of similar geomorphological setting are the Mekong River, Cambodia (Richards et al., 2018); Red River, Vietnam (Berg et al., 2007; Postma et al., 2012, 2016; Stopelli et al., 2020; Trung et al., 2020; Wallis et al., 2020), Pearl River, China (Huang et al., 2011); Hetao Basin, Inner Mongolia (Guo et al., 2008; Cao et al., 2018), Río Dulce, Argentina (Bundschuh et al., 2004; Bhattacharya et al., 2006), Pazña River, Bolivia (Ramos et al., 2014), Lower Katari Basin, Bolivian Altiplano (Quino Lima et al., 2021).

The source of arsenic enrichment in shallow Holocene aquifers is linked to infiltration of dissolved arsenic from river water to aquifer in the depositional basin (Postma et al., 2016; Trung et al., 2020), and to the *in-situ* microbially-steered reductive dissolution of arsenic (Ghosh and Bhadury, 2018; Ghosh et al., 2021) from, e.g., biotite (Seddique et al., 2008); iron-oxyhydroxides (Nickson et al., 1998), arsenic-bearing pyrites and arsenopyrites (Acharyya et al., 2000, 2007; Shah, 2017). Mukherjee et al. (2019) presented a comprehensive overview in which the worldwide occurrence of arsenic pollution in the shallow-aquifer domain of Holocene foreland basins is linked to primary arsenic sources in mountain belts of convergent continental margins in Alpine and older orogenic systems. Documented primary natural arsenic sources are, among others, volcanic rocks, salts and thermal waters (Tapia et al., 2019), arsenic-enriched magmatic rocks (Mukherjee et al., 2014), brecciated marbles (Göd and Zemann, 2000), hydrothermal arsenic enrichment of calcite veins in altered fault rocks (Horton et al., 2001; Campbell et al., 2004). Upon weathering of the orogenic rocks, the arsenic that is chemically-bound to rock fragments is river-transported to the sedimentary sink, where it is deposited as part of the siliciclastic alluvial-basin sediment.

The geomorphological juxtaposition of (a) compacted, low-porosity

and low-permeability, organic matter-rich clay silt and clay deposits in abandoned and sediment-filled meandering-river bends (or: *clay-plugs*), and (b) high-porosity, high-permeability sandy point-bar deposits (see: Graphical Abstract) forms a dynamic combination in which microbially-steered reductive desorption of arsenic takes place in the anoxic clay-plug environment (Ghosh et al., 2021). Biogeochemical factors such as redox conditions, pH, presence of different ions and metabolic activity of indigenous microbial communities play a crucial role in the mobilization of arsenic (Islam et al., 2004; Harvey et al., 2006; Bhattacharya et al., 2007; Ghosh et al., 2015a, 2021). The desorbed arsenic subsequently migrates along the porosity–permeability gradient into the adjacent sandy point-bar aquifer (Donselaar et al., 2017; Ghosh et al., 2021), where it is stratigraphically entrapped by the permeability contrast with the surrounding fine-grained alluvial-plain and clay-plug sediment (Donselaar and Overeem, 2008; Weinman et al, 2008; Sahu and Saha, 2015; Donselaar et al., 2017; Jakobsen et al., 2018).

To get to grips with the magnitude of the pollution problem, the present paper aims to quantify the total arsenic volume contained in clay-plug sediment, and that can potentially be desorbed in the anoxic clay-plug environment, and migrate to the point-bar aquifer. To reach the aim, the arsenic content of sediment samples was analysed from five shallow (15 to 50 m depth), fully-cored wells, drilled in Holocene clay-plug and point-bar sediment along the Ganges River in Bihar, India. The quantitative data set was complemented with published data (Ghosh et al., 2015b) on arsenic concentrations in clay-plug sediment in the Nadia District in West Bengal (India). Next, the concentration values were assigned to the clay-plug bulk sediment volumes as calculated from Sentinel-2 satellite surface area data in combination with side-scan sonar depth profiling of oxbow lakes and the Ganges River, and sedimentological data from the cored wells. The results of the study provide a quantitative data set on potential arsenic availability in the shallow aquifer domain, which is vital to envisage the magnitude of the pollution problem, and to develop mitigation strategy models accordingly.

2. Geomorphological setting

The study area is in the alluvial plain of the Ganges River in the Middle Ganges Plain (MGP) in Uttar Pradesh and Bihar (India) (Fig. 1A-B), part of the larger Indo-Gangetic foreland basin between Peninsular India in the south and the Himalayas in the north. The alluvial landscape in the MGP is shaped by Holocene floodplain and meandering-river deposits of the Ganges River and its tributaries. The process of chute-channel shortcutting (Bridge, 2003; Nichols, 2009) has detached meander loops from the active river and converted these crescent-shaped oxbow lakes (Fig. 1C–D), where hydrophytes and animal life thrive in the standing bodies of lake water, and contribute to the high rates of organic matter deposition into the lake sediment (Lawson et al., 2013; Ghosh and Biswas, 2015; Ghosh et al., 2021). Oxbow lakes eventually fill-in with sediment by aggradation of a mixture of organic debris and clay and silt that settles out of suspension from the lake water column and, upon completion of the infill process, convert to so-called clay plugs (Fig. 1D). The clay and silt easily compact, and are characterized by very-low porosity and permeability. In the active river period, prior to meander-loop cut-off, sand is accumulated by bed-load sediment transport in point bars on the inner river bends (Bridge, 2003). The sandy point-bar deposits are characterized by high porosity and permeability values (Hartkamp-Bakker and Donselaar, 1993), that strongly contrast with the surrounding clay-plug and floodplain fines, and result in differential compaction where the point-bars stand out as a positive relief in the flat and clay-dominated alluvial-plain landscape. Human settlements are concentrated on the point bars because the elevated position is a protection against seasonal monsoonal river flooding. In the study area, piped water-supply grids are absent, and groundwater for consumption and irrigation is directly extracted from the point-bar aquifer by hand-pump wells of approximately 30 m depth (Donselaar et al., 2017).

Table 1
Coordinates of the data used in this study.

	Latitude	Longitude		Latitude	Longitude
Clay plugs			**Clay plugs**		
01	25°39.338′N	84°39.878′E	11	25°28.929′N	83°37.250′E
02	25°37.632′N	84°39.144′E	12	25°25.736′N	83°14.333′E
03	25°35.237′N	84°31.484′E	13	25°43.618′N	85°3.302′E
04	25°50.625′N	84°43.770′E	14	25°28.175′N	84°50.625′E
05	26°3.920′N	84°53.511′E	15	25°33.311′N	85°21.003′E
06	26°4.186′N	84°13.224′E	16	25°34.436′N	85°53.191′E
07	25°50.589′N	84°19.684′E	17	25°33.783′N	85°52.170′E
08	25°37.661′N	84°11.903′E	18	25°40.603′N	86°17.828′E
09	25°35.534′N	84°8.018′E	19	25°49.746′N	87°20.696′E
10	25°41.437′N	83°53.356′E	20	25°30.621′N	87°35.628′E
Wells			**Side scan sonar surveys**		
BKP-1	25°40.014′N	84°40.913′E	01	25°40.747′N	84°42.474′E
BKP-2	25°39.551′N	84°40.565′E	02	25°41.868′N	84°36.010′E
BKP-3	25°39.037′N	84°40.064′E	03	25°38.901′N	84°24.156′E
BKP-4	25°39.102′N	84°41.811′E	04	25°38.214′N	84°18.846′E
SHY-1	25°39.230′N	84°23.602′E			

3. Data and methods

Remote sensing and ground-truth geomorphological and sedimentological data sets were collected along the alluvial plain of the Ganges River (Fig. 1; Table 1). Sedimentological descriptions from five shallow (15 to 50 m depth), fully-cored wells provided details of the point-bar and clay-plug lithofacies succession (Fig. 1C,D). In total 36 sediment samples were recovered from the cores for further analyses. Samples were stored in individual zip-lock polyethylene bags for analyses of total organic carbon (TOC), elemental extraction and quantification with inductively coupled mass spectrometer (ICP-MS). The methodology of Bojko and Kabala (2014) was followed for TOC analysis, and the Swedish Standard Method (SIS, 1993) for the elemental extraction. For the latter, sample digestion was carried out by treating about 0.5 g dried sediment sample with 10 ml 7 M HNO_3 at 100 kPa and 121 °C for 30 min. The solution was cooled down and centrifuged at 14,000 RCF for 15 min. The CRM-601 standard was used as a certified reference sediment to calculate the errors. The extracts were diluted before analysing the elemental levels in an inductively coupled mass spectrometer (ICP-MS-Thermo Scientific X-Series II).

As a first step for the estimation of potential arsenic volume in clay plug sediments, the bulk volume of clay plugs was calculated (Fig. 2 and Graphical Abstract) by multiplying (1) the surface areas of twenty clay plugs, extracted from Sentinel-2 satellite images (Fig. 1A) with (2) cross-sectional shape models from four side-scan sonar surveys across oxbow lakes and the Ganges River (Fig. 1B, 3). Next, sediment proportion ratios of the three sediment classes (clay, silt and sand) from own core data and from three complementary cored well data sets (Ghosh et al., 2015b, 2017) were used to assign (3) bulk sediment volumes to the clay plugs. The ICP-MS analysis results gave the solid-state arsenic content in each of the three sediment classes, and this allowed to (4) calculate the potential arsenic volume in each of the clay plugs.

3.1. Clay-plug surface area

Surface areas of twenty clay plugs were extracted from Sentinel-2 satellite raster images with ArcGIS. Sentinel-2 multispectral band data ranging from 0.49 μm to 1.00 μm (visible light to Near Infrared) with 10 m spatial resolution were used for self-iterated unsupervised classification in ArcGIS. The output was rectified with a 3x3 edge-detection filter. The unsupervised raster images were converted to vector data in ArcGIS for automated calculation of the surface areas. Data consistency was cross-verified with Google Earth-Pro images.

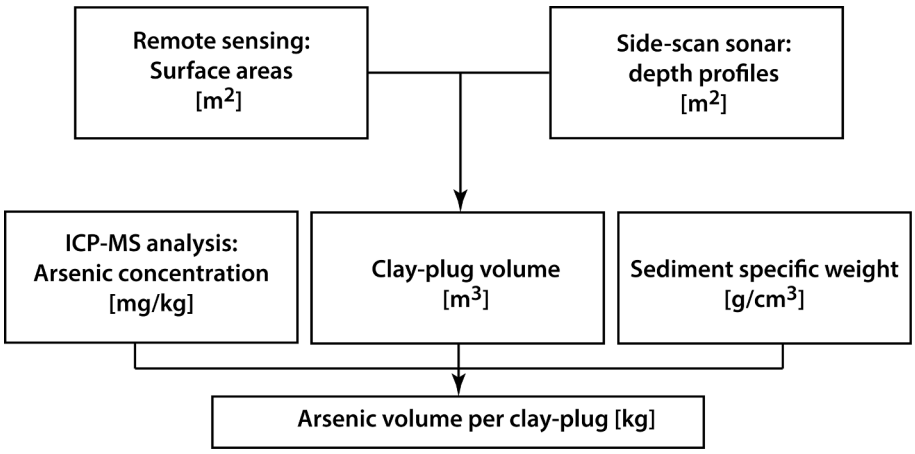

Fig. 2. Flow chart for the calculation of arsenic content in the clay plugs.

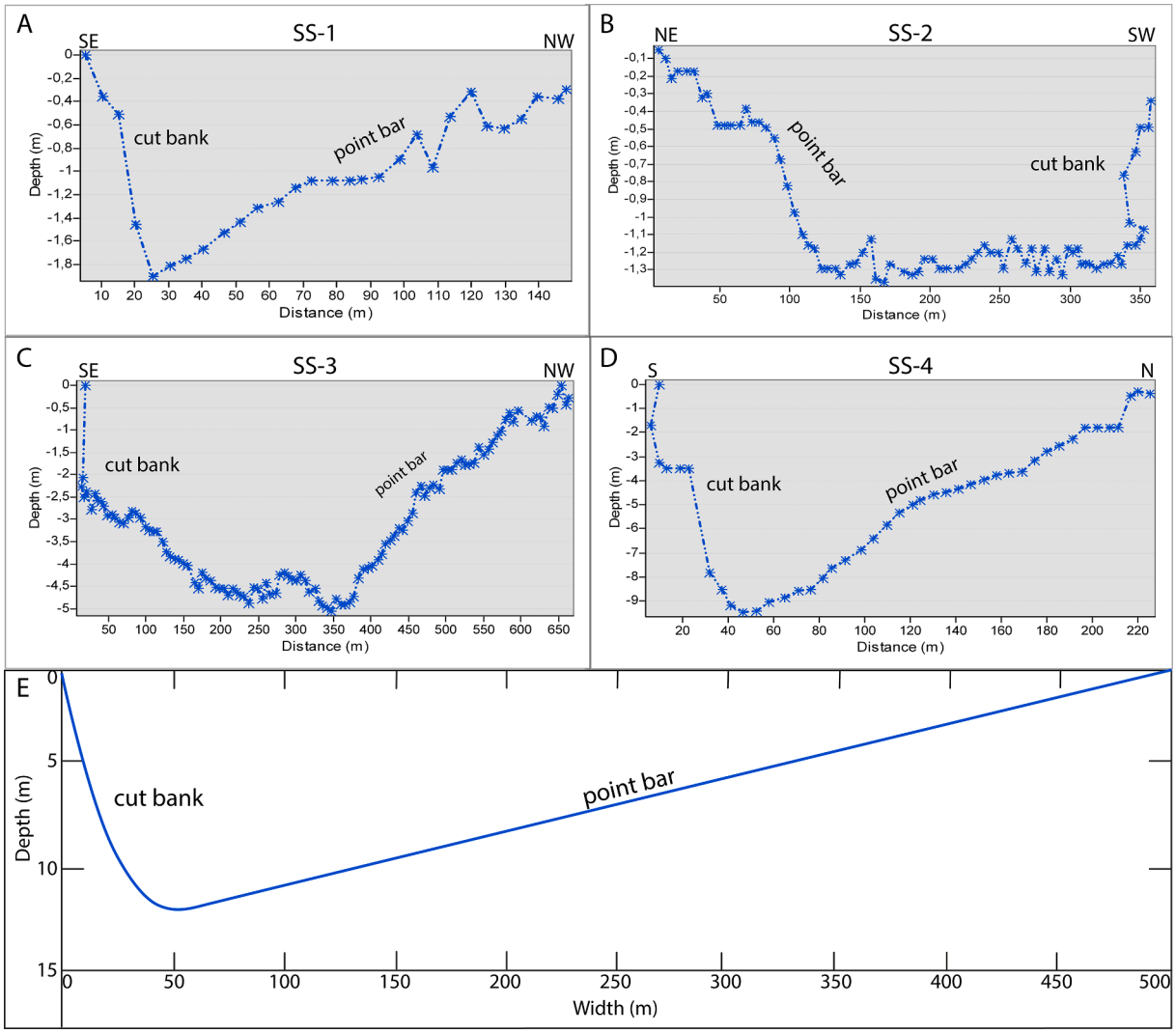

Fig. 3. A-D: Side-scan sonar profiles SS-1 to SS-4. See Fig. 1 for profile locations. E: Synthetic cross profile based on the side-scan sonar and core data.

3.2. Clay-plug cross-sectional area calculations

Four side-scan sonar surveys across the oxbow lakes and Ganges River served to generate the cross-sectional depth profile model for clay plugs. The asymmetric profiles (Fig. 3A–D) with a steep outer bank (or: *cut bank*) near the channel thalweg, and a gently sloping inner bank (or: *point bar*), were converted in MATLAB to a parabolic synthetic cross section (Fig. 3E). To assign the clay-plug thickness to the cross-section, the total height difference between channel thalweg and top of the point bar (or: bank-full depth) was measured. The largest measured present-

Table 2
Bulk density values of the clay-plug sediment.

BKP-4		Average	
Thickness (m)	% of total thickness	% of total thickness ((a + b)/2)	Fraction
7.2	73.47	63.62	0.636
2.2	22.45	14.05	0.141
0.4	4.08	22.32	0.223

Sediment type	Average (grain fraction)	Rho (Density)kg/m^3	Mean Eff. Porostity (%)	Mean eff. bulk density (fraction)
Clay	0.636	1200	0.06	0.60
Silt	0.141	1280	0.20	0.11
Sand	0.223	1520	0.32	0.15
Water		1000		0.14
	Rho(Eff.)	1230.03		

day channel depth measured with side-scan sonar is 9.5 m in profile SS-4 (Fig. 2B, 3D). A Jacob's staff survey yielded a height difference of 2.5 m from the waterline to the top of the point bar at the location of SS-4 (Fig. 2B), which gives the total height of 12 m from channel thalweg to point-bar top. The height was corroborated by the clay-plug thickness in wells BKP-3 and BKP-4 (Fig. 1D, 4). Similar thicknesses were described by Ghosh et al. (2015b) and Ghosh et al., (2017) in wells through clay plugs on the alluvial plain of the Ganges River in West Bengal (India). For the cross-sectional area calculations, the width of the synthetic cross-sectional profile was scaled to the measured width in ArcGIS of each individual clay-plug; the depth was fixed at 12 m, assuming that the scouring depth of the Ganges River is constant in the along-river equilibrium profile in the low-gradient part of the MGP. The synthetic cross profiles, in combination with the clay-plug surface radius were used to calculate the contact area between the clay plug and the point bar.

3.3. Bulk sediment weight

As a next step, the calculated clay plug bulk volume was converted to bulk sediment weight. The sedimentological logs of the two wells penetrating the clay plugs (BKP-3 and BKP-4; Fig. 1D, 4) provided the ratio of the different sediment types in the clay plugs. The sediments were deposited in the standing body of oxbow lake water, and therefore it is assumed that the sediments are fully water-saturated and the pore spaces are filled with water (Bear, 1972). Standard specific weight values for sand, silt and clay (Hillel, 1980; Linsley et al., 1982; Yu et al., 1993), and average effective porosity values for unconsolidated sediment (McWhorter and Sunada, 1977) were assigned for the calculations (Table 2). Porosity values for coarse, medium and fine sand were grouped, because of their close similarity in porosity and permeability (Freeze and Cherry, 1979). The initial porosity, i.e., before compaction, of clay-rich sediments ranges from 40% to 95% (Holbrook, 2001). For clay-rich sediments in oxbow lakes, initial porosities range from 70% to 90% (Singer and Müller, 1983). The initial porosity of unconsolidated sand varies from 35% to 50% (Stone and Siever, 1996). As the sediments in the cores showed compaction, the average values of representative porosity for compacted sand, clay and silt as described by Yu et al. (1993) were used in the present calculations.

The bulk density ρ_{bulk} is calculated as:

$$\rho_{bulk} = [((1-\varphi_{clay})*clay\%)*\rho_{clay}] + [((1-\varphi_{silt})*silt\%)*\rho_{silt}] + [((1-\varphi_{sand})*sand\%)*\rho_{sand}] + [\{(\varphi_{clay}*clay\%) + (\varphi_{silt}*silt\%) + (\varphi_{sand}*sand\%)\}*\rho_{water}] \quad (1)$$

Table 3
Arsenic and iron elemental concentrations, and the correlation coefficient between both elements.

BKP-2		
Depth (m)	*As (mg/kg)	*Fe (g/kg)
1.3–1.4	36.827	191.100
2.7–2.8	16.458	101.390
4.9–5.0	13.815	41.270
8.0–8.1	14.162	50.650
11.5–11.6	23.739	109.809
12.2–12.3	7.702	67.060
12.9–13.0	4.140	40.384
13.6–13.7	4.272	37.106
15.7–15.8	2.069	36.345
17.8–17.9	3.036	35.437
20.6–20.7	2.871	31.698
22.7–22.8	4.773	38.178
24.8–24.9	3.205	50.979
28.3–28.4	3.663	57.544
29.7–29.8	1.625	33.815
30.4–30.5	1.660	34.499
33.2–33.3	0.605	18.579
34.6–34.7	1.240	27.884
Correlation coefficient BKP-2	**0.932**	
BKP-4		
Depth (m)	***As (mg/kg)**	***Fe (g/kg)**
2.7–2.8	26.939	382.689
6.2–6.3	29.388	175.017
11.1–11.2	19.768	76.046
13.9–14.0	16.588	84.385
17.4–17.5	8.340	72.588
20.9–21.0	6.986	65.217
25.1–25.2	6.235	66.376
26.5–26.6	6.123	64.350
28.6–28.7	2.235	56.380
30.7–30.8	25.003	166.188
32.8–32.9	0.589	52.743
34.9–35.0	4.300	26.589
Correlation coefficient BKP-4	**0.753**	
SHY-1		
Depth (m)	***As (mg/kg)**	***Fe (g/kg)**
5.1–5.2	38.913	211.102
10.0–10.1	39.133	207.975
11.4–11.5	31.486	127.606
12.8–12.9	19.460	102.801
14.4–14.5	19.202	84.755
15.6–15.7	13.845	79.926
Correlation coefficient SHY-1	**0.955**	

in which φ is the porosity, and clay%, silt% and sand% the specific-weight values.

The total weight of a clay plug (W) is calculated as:

$$Clay-plugweight(W) = Clay-plugvolume(V)*\rho_{bulk} \quad (2)$$

3.4. Arsenic weight per clay plug

Elemental analysis (ICP-MS based) of four core samples from the clay-plug intervals in wells BKP-4 and SHY-1 (Fig. 1C-D) yielded the arsenic weight fraction in the sediments (Table 3; Fig. 5). The average arsenic content from the samples in the upper clay plug interval (12 m in wells BKP-4, and 8 m in SHY-1; Fig. 4) was calculated, and this value was used to calculate the total potential arsenic weight per clay plug:

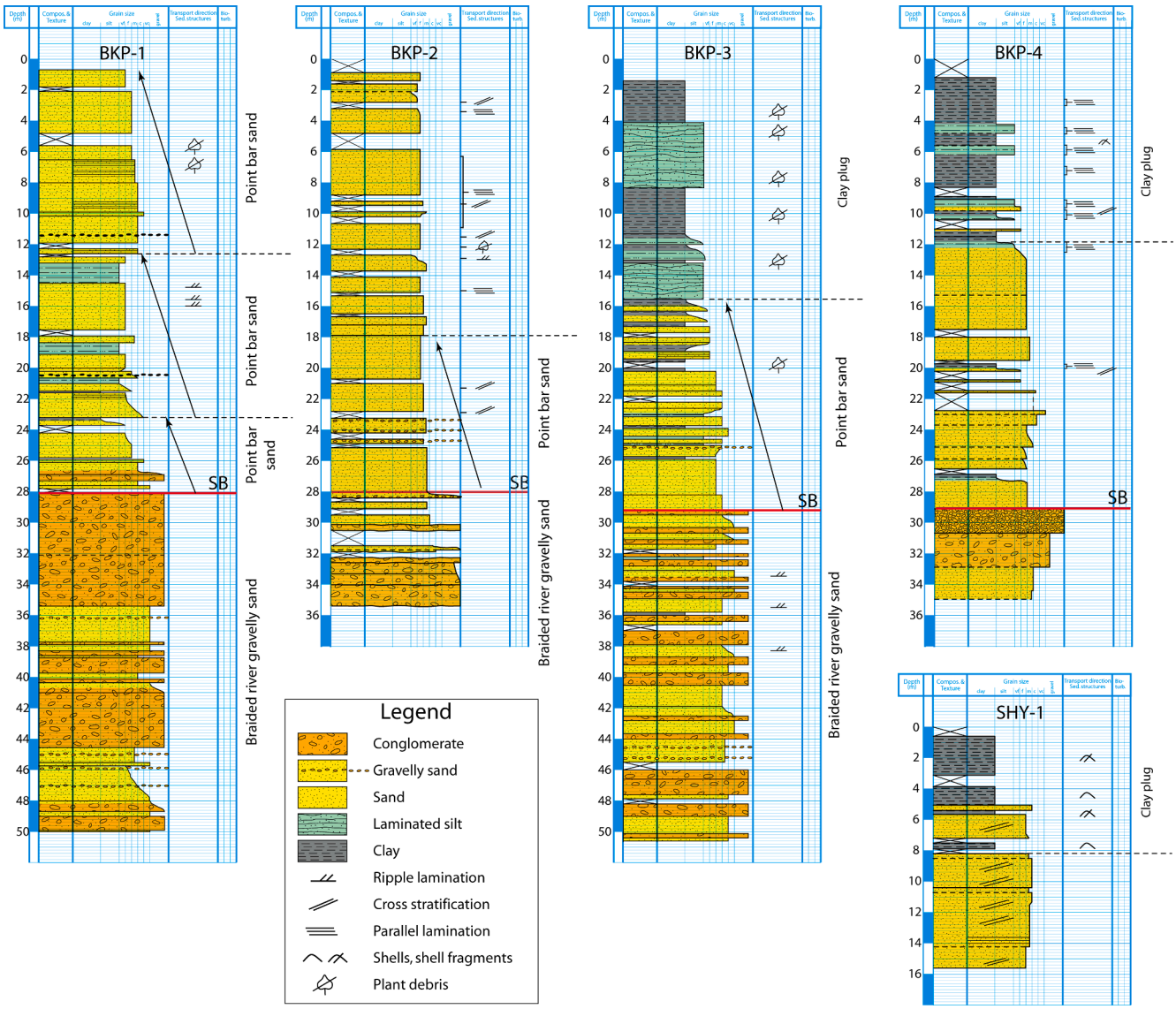

Fig. 4. Sedimentological logs BKP-1 to BKP-4, SHY-1. See Fig. 1C-D for well locations.

$$Arsenic\ \ weight = clay - plug\ \ weight * Average\ \ As\ \ concentration \quad (3)$$

4. Results

The twenty clay plugs in the study area have a wide variety in surface area, ranging from 0.42 $\cdot 10^6$ m^2 to 18.78 $\cdot$ 10^6 m^2 (Table 4) and, consequently, the total sediment volume of the individual clay plugs varies between 2.44 $\cdot$ 10^6 m^3 and 113.01 $\cdot$ 10^6 m^3. The total solid-state arsenic weight contained in the clay plug sediment is calculated from the average content of wells BKP-4 and SHY-1 clay-plug samples of 28.75 mg/kg, and amounts to 0.07 $\cdot$ 10^6 kg to 3.13 $\cdot$ 10^6 kg per clay plug (Table 4). The arsenic and iron content in the wells show a decrease with depth (Fig. 5), with a correlation coefficient between both elements of more than 0.9 in wells BKP-2 and SHY-1. This is consistent with earlier studies (Ghosh et al., 2015b), which suggest that the geogenic arsenic in this region is mostly present in the form of arsenic-bearing iron minerals such as pyrite, Fe-(hydro)oxides (Mukherjee et al., 2011). The lower correlation coefficient of 0.75 in well BKP-4 is cause by a spike in arsenic and iron content in highly porous and permeable unconsolidated conglomerate at 30.7–30.8 m, just below the sequence boundary with overlying low-permeable, fine-grained sand (Donselaar et al., 2017, Kumar et al., 2019). A similar trend of decrease with depth is observed in the TOC content in wells BKP-2, BKP-4 and SHY-1, with again a spike below the sequence boundary in BKP-4 (Fig. 6).

The measured arsenic concentrations in the clay-plug samples ranges from 19.8 to 38.9 mg/kg and is in the range of published data of arsenic concentrations in sediment cores. Bundschuh et al. (2004) reported arsenic concentrations of 6 mg/kg in the upper 20 m of the fluvial sedimentary strata of Chaco-Pampean Plain (Argentina); Zheng et al. (2005) reported values up to 14 mg/kg in the upper 20 m of the Dari well in Holocene Meghna River floodplain sediments in Araihazar, Bangladesh; Berg et al. (2007) documented arsenic concentration ranges from 2 to 33 mg/kg in Holocene sediments of the Red River Delta, Cambodia and Vietnam; in two of the three published wells the arsenic concentrations sharply decrease below approximately 15–20 m depth. Ghosh et al. (2015b) documented arsenic concentrations in 12-m-thick Holocene clay-plug sediment of Nadia District in West Bengal (India) that range from 2 to 21 mg/kg. Seddique et al. (2008) reported arsenic concentrations of 0 to 12 mg/kg (with an outlier of 53.4 mg/kg) in Holocene Meghna River sediment.

5. Discussion

Spot measurements in Holocene aquifers highlight the heterogeneity

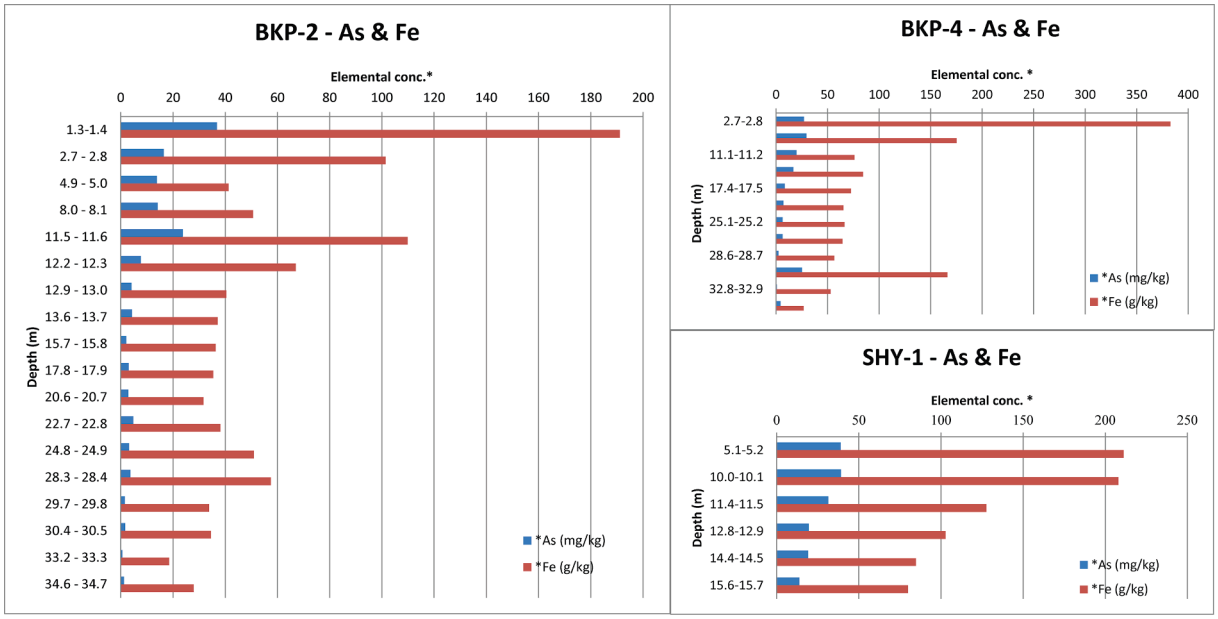

Fig. 5. Arsenic and iron concentrations in wells BKP-2, BKP-4 and SHY-1. See Fig. 1C-D for well locations.

Table 4
As-volumes of all clay plugs.

Clay plug	Clay Plug Area (10^6 m^2)	Clay Plug Volume 10^6 m^3	As weight (10^6 kg)	Contact Area (10^6 m^2)	Arsenic load (kg/m^2)
1	14.95	81.63	2.26	15.17	0.149
2	11.75	65.38	1.81	11.35	0.160
3	16.64	85.85	2.38	14.56	0.163
4	1.92	10.71	0.30	1.95	0.152
5	0.42	2.44	0.07	0.41	0.164
6	2.70	15.09	0.42	2.69	0.155
7	6.17	34.70	0.96	5.86	0.164
8	9.50	49.08	1.36	9.47	0.144
9	18.78	113.01	3.13	21.80	0.144
10	3.70	24.89	0.69	4.34	0.159
11	15.14	57.12	1.58	10.58	0.150
12	15.18	83.64	2.32	13.24	0.175
13	4.25	22.03	0.61	4.50	0.136
14	3.36	19.92	0.55	3.45	0.160
15	5.92	34.30	0.95	6.58	0.144
16	14.82	78.32	2.17	14.02	0.155
17	17.59	91.76	2.54	16.60	0.153
18	2.65	17.91	0.50	3.24	0.153
19	0.96	5.12	0.14	0.93	0.153
20	1.25	10.49	0.29	1.84	0.158

of arsenic pollution concentrations, both on the surface, as with depth (e.g., Bundschuh et al., 2004; Zheng et al., 2005; Acharyya and Shah, 2007; Berg et al., 2007; Seddique et al., 2008; Shah, 2008, 2010, 2017; Ghosh et al., 2015b; Sahu and Saha, 2015; Donselaar et al., 2017, Jakobsen et al., 2018). In this paper the concentrations have been extrapolated to total arsenic load contained in a single clay-plug morphological element. The total load is considered here as static, and no recharge by introduction of additional arsenic into the clay plug is taken into consideration. The remaining questions are: (a) whether the bulk of the arsenic that is adsorbed to sediment grains in the clay plug, has potential of release and migration to the aquifer waters, and (b) the nature of migration of the released arsenic from low-porosity, low permeability clay-plug sediment to the aquifer domain in the adjacent porous and permeable point-bar sand.

5.1. Arsenic release

Arsenic release is driven by microbial reduction and mobilization of arsenic associated with iron-oxy(hydroxide) minerals (Ghosh et al., 2015a, 2021). Microbial metabolism is controlled by the availability of organic carbon (OC). The sandy alluvial sediments are generally lean in OC. By contrast, clay-plug sediment in the study area has high TOC concentrations of 0.7–0.8% in wells BKP-4 and SHY-1 (Fig. 6). Ghosh et al. (2015a) reported similar TOC concentrations (of 0.7%) in clay-plug deposits at depths to12 m in Haringhata (Nadia district, West Bengal, India). The presence of high macrophytes growth coverage in the oxbow lake (Ghosh and Biswas, 2015; Ghosh et al., 2021) blocks the penetration of light, and prevents water circulation in the lower part of the water column in the oxbow lake, and contributes to the development of an anaerobic environment in the hypolimnion favourable for the desorption of As from FeOOH (e.g., Bhattacharya et al., 2002). Decayed oxbow-lake macrophytes are the source of TOC, and are considered vital for the metabolism process (Ghosh et al., 2017, 2021). The OC associated with the sediment provides nutrition to the microorganisms (bacteria) in the system (Ghosh et al., 2015a). During the heterotrophic metabolism in anaerobic or facultative aerobic environment, the organic molecules act as electron donors and this subsequently reduces the arsenate [As(V)] which enters into the microbial cell via Pit transporters and converted to arsenate [As(III)] by arsenate reductase enzymes within the cell, and then released into the environment (Fig. 7). The gradual decrease of OC coupled with decreased arsenic and iron concentrations in the sediment with depth below the clay plugs (Fig. 6) testifies to the effectiveness of the arsenate reduction process.

5.2. Arsenic transfer by diffusion and advection

5.2.1. Diffusion process in the clay plug

Under the assumption that microbially-steered reductive dissolution of arsenic is effective in the anoxic clay-plug environment, diffusion is the principal process of arsenic expulsion in the gravitational, compaction-driven environment, and advection transport driven by concentration differences takes over in the adjacent point-bar sand past the permeability boundary at the clay-plug to point-bar interface. Because of the permeability anisotropy between the very low-permeable, compacted clay sediment and the porous and permeable point-bar sands, discharge of dissolved arsenic will be directed towards

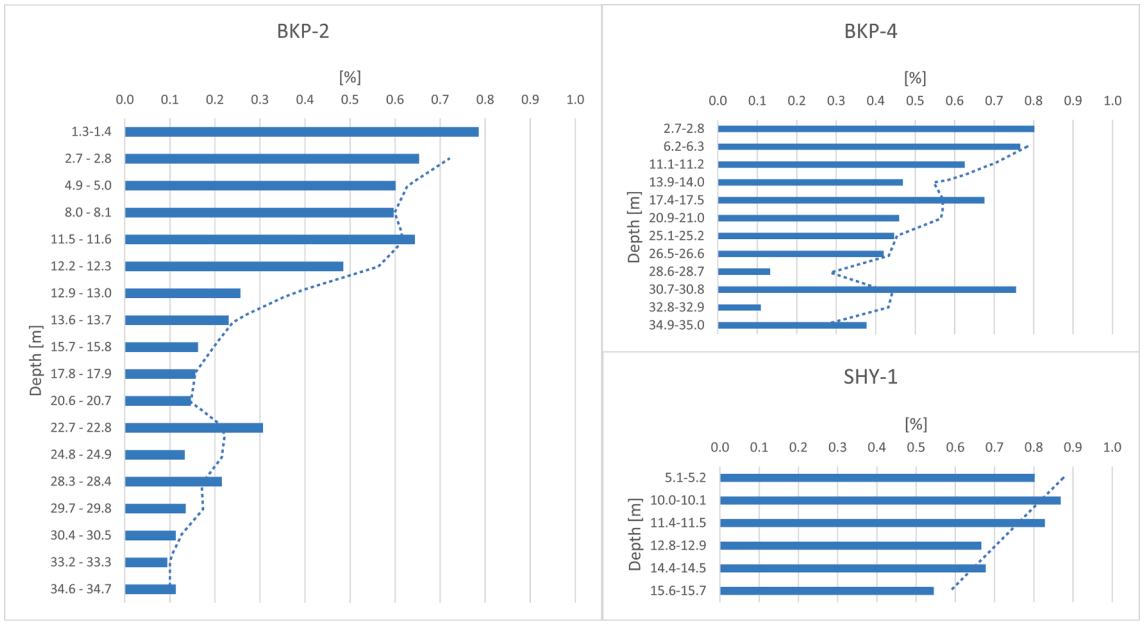

Fig. 6. TOC content in the core samples of wells BKP-2, BKP-4, SHY-1. Dashed lines: moving average (period = 2) trend line. See Fig. 1C-D for well locations.

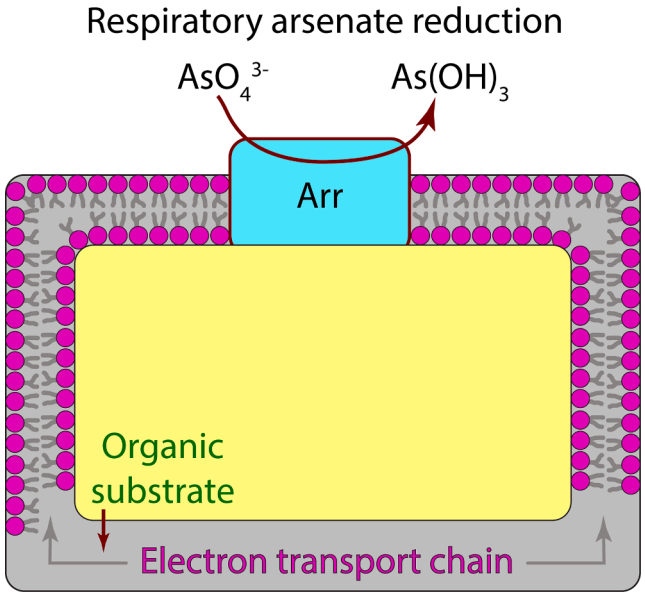

Fig. 7. Schematic model for microbial respiratory arsenate reduction and mobilization.

the clay-plug – point-bar interface by the process of diffusion. The hydraulic conductivity is linearly related to the diffusion flux. The arsenic released in the clay plug by metabolic arsenate reduction leads to accumulation with respect to the adjacent point-bar sand. At the interface of the compacted, low-permeable clay and the highly permeable point-bar sand, arsenic transport occurs through molecular diffusion which levels the concentrations of arsenic by redistributing elements with higher concentration to elements with lower concentration (Bear, 1972; Kumar et al., 2019). Once the reduced arsenic molecules enter the permeable point-bar sand, advection is the process through which transport of arsenic occurs within the aquifer system along the pressure gradient. The latter is amplified by water extraction through the hand-pump wells.

To get to grips with the potential of dissolved arsenic diffusion volume along the permeability gradient and across the permeability interface, the contact area between the clay plug and bordering point-bar sand was calculated in MATLAB. It is assumed that the arsenic in the clay plug is not replenished, and that the amount and discharge will decrease exponentially over time. For the estimate of the diffusion flux, Fick's first law of diffusion is used (Eq. (4)) with two assumptions, firstly that the system is in a steady-state, and secondly that the medium is homogeneous.

$$J = -D\nabla C \tag{4}$$

D is the diffusion coefficient, a material-specific property, and C is the concentration. With some modifications, Fick's first law for transport through a membrane is given by Eq. (5):

$$J = K\Delta C \tag{5}$$

where J is diffusion flux [mol $m^{-2}s^{-1}$], K the hydraulic conductivity of the medium [m s^{-1}] and ΔC the difference in concentration [mol m^{-3}]. In the hydraulic conductivity, crucial to the modified version of Fick's first law, the following range was used: a minimal hydraulic conductivity of 10^{-8} ms^{-1} and maximal value of 10^{-7} ms^{-1} (Bear, 1972). The results of the calculations are that – with contact area between the clay plug and the adjacent point bar varying between $0.41 \cdot 10^6$ m^2 and $21.80 \cdot 10^6$ m^2 – the potential dissolved arsenic load that could pass through the contact area amounts to 0.136 – 0.175 kg/m^2. The initial diffusion flux through the contact area, based on the application of Fick's First Law, ranges between 10^1 and 10^2 g/(m^2 y^{-1}).

5.2.2. *Point-bar advective flow along the pressure gradient*

The lithofacies distribution of point-bar deposits is characterized by the presence of (a) high-permeable clean sand lag deposits at the base (which in hydrocarbon enhanced recovery scenarios are referred to as so-called 'thief zones', (b) fining-upward grain-size sequences towards the top of the point-bar sediment body, that form as response to the energy anisotropy of the helicoidal flow in the meandering-river bend, and (c) inclined clayey lateral accretion surfaces in the upper two-thirds of the point-bar morphology that form in peak runoff periods when the river water expands over the adjacent alluvial plain (see the Graphical Abstract; Hartkamp-Bakker and Donselaar, 1993; Donselaar and Overeem, 2008). This very specific spatial arrangement of sedimentological and related poro-perm characteristics determines the direction of advective fluid flow and transport of dissolved arsenic in the aquifer

system beyond the clay-plug – point-bar interface. Flow direction is along the thief zone at the base of the point-bar sediment body, and up the point-bar slope along the pressure gradient formed by water extraction through hand-pump wells by the villagers living on the elevated point-bars (see the dashed lines with arrows in the Graphical Abstract) and, consequently, draws the arsenic-polluted water to the well-head, thereby aggravating the pollution problem for the inhabitants.

6. Conclusions

With the aim to understand the magnitude of the arsenic-pollution problem in the shallow-aquifer domain of Holocene meandering-river geomorphology, the potential total arsenic load contained in clay-plug sediment was calculated by the integrated analysis of bulk sediment volume of twenty clay plugs (i.e., abandoned and sediment-filled meandering-river bends) in the Holocene alluvial plain of the Ganges River in Bihar, India with (a) remote-sensing imagery analysis of the clay-plug surface area, (b) four side-scan sonar surveys in present-day oxbow lakes and in the active Ganges River for the calculation of clay-plug cross-sectional area, (c) sedimentological data of five fully-cored wells in clay plugs, point-bar sand, and a partly-filled oxbow lake, all in Bihar, complemented with sediment-type and arsenic content data from three wells in Haringhata, West Bengal, India, and (d) Elemental (ICP-MS based) data of arsenic distribution in the sediment columns. The total arsenic load stored in sediment of individual clay plugs was calculated to range from $0.07 \cdot 10^6$ kg to a staggering $3.13 \cdot 10^6$ kg, depending on the size of the clay plug. The juxtaposition of clay-plug and point-bar geomorphological elements with their lithofacies differences and inherent porosity and permeability anisotropy, is proposed as a recipe for arsenic release, transport and storage. Based on the arsenic, iron and TOC concentration trends in the boreholes, a scenario is presented for the desorption of arsenic by the process of respiratory arsenate reduction by microbial metabolism, which is favoured by the high TOC concentrations in clay-plug sediment. The released arsenic is transported to the interface between low-permeable clay-plug sediment and high-permeable point-bar sand by the process of molecule diffusion. The initial diffusion flux across the interface ranges between 10^1 and 10^2 $g/(m^2\,y^{-1})$. Direction of advective fluid flow and arsenic transport in the adjacent point-bar sediment body is conditioned by the lithofacies distribution and intricate porosity and permeability anisotropy. Water extraction by hand-pump wells creates a pressure gradient in the point-bar aquifer system, and draws the arsenic-polluted water to the well-head.

Declaration of Competing Interest

The authors declare that they have no known competing financial interests or personal relationships that could have appeared to influence the work reported in this paper.

Acknowledgements

Financial support for this study from the NWO-WOTRO research program “Urbanizing Deltas of the World” (UDW Grant No. W 07.69.205), and from the Department of Science and Technology, Gov. of India (INSPIRE Faculty Grant No. DST/INSPIRE/04/2015/002362) is gratefully acknowledged. The authors are indebted to the Bihar State Pollution Control Board and to AN College, Patna for providing the core description facilities. Abhinaba Das (Indian Institute of Science, Bengaluru) helped in sample analyses. The authors enjoyed the discussions on arsenic mitigation with our partners in the NWO-WOTRO DELTAP project: Doris van Halem, Annemarie Mink and Muhammad Annaduzzaman (TU Delft), Bilqis Hoque (ERPC, Dhaka, Bangladesh). Two anonymous reviewers are thanked for their constructive comments.

References

Acharyya, S.K., Lahiri, S., Raymahashay, B.C., Bhowmik, A., 2000. Arsenic toxicity of groundwater in parts of the Bengal basin in India and Bangladesh: the role of Quaternary stratigraphy and Holocene sea-level fluctuation. Environ. Geol. 39, 1127–1137. https://doi.org/10.1007/s002540000107.

Acharyya, S.K., Shah, B.A., 2007. Groundwater arsenic contamination affecting different geologic domains in India—a review: influence of geological setting, fluvial geomorphology and Quaternary stratigraphy. J. Environ. Sci. Heal. A. 42, 1795–1805. https://doi.org/10.1080/10934520701566744.

Ahmed, K.M., Bhattacharya, P., Hasan, M.A., Akhter, S.H., Alam, S.M.M., Bhuyian, M.A. H., Imam, M.B., Khan, A.A., Sracek, O., 2004. Arsenic enrichment in groundwater of the alluvial aquifers in Bangladesh: An overview. Appl. Geochem. 19, 181–200. https://doi.org/10.1016/j.apgeochem.2003.09.006.

Bear, J., 1972. Dynamics of Fluids in Porous Media. Elsevier, New York, USA.

Berg, M., Stengel, C., Trang, P.T.K., Hung Viet, P., Sampson, M.L., Leng, M., Samreth, S., Fredericks, D., 2007. Magnitude of arsenic pollution in the Mekong and Red River Deltas - Cambodia and Vietnam. Sci. Total Environ. 372, 413–425. https://doi.org/10.1016/j.scitotenv.2006.09.010.

BGS, DPHE, 2001. Arsenic Contamination of Groundwater in Bangladesh, in: Kinniburgh, D.G., & Smedley, P.L. (Eds.), Br. Geol. Surv. Rep. WC/00/19, Br. Geol. Surv. 1. Keyworth, UK, 1–21.

Bhattacharya, P., Chatterjee, D., Jacks, G., 1997. Occurrence of arsenic-contaminated groundwater in alluvial aquifers from delta plains, eastern India: Options for safe drinking water supply. Int. J. Water Resour. Dev. 13, 79–92. https://doi.org/10.1080/07900629749944.

Bhattacharya, P., Claesson, M., Bundschuh, J., Sracek, O., Fagerberg, J., Jacks, G., Martin, R.A., Storniolo, A., Thir, J.M., 2006. Distribution and mobility of arsenic in the Río Dulce alluvial aquifers in Santiago del Estero Province. Argentina. Sci. Total Environ. 358, 97–120. https://doi.org/10.1016/j.scitotenv.2005.04.048.

Bhattacharya, P., Jacks, G., Ahmed, K.M., Routh, J., Khan, A.A., 2002. Arsenic in groundwater of the Bengal Delta Plain aquifers in Bangladesh. Bull Environ. Contam. Toxicol. 69, 538–545. https://doi.org/10.1007/s00128-002-0095-5.

Bhattacharya, P., Welch, A.H., Stollenwerk, K.G., McLaughlin, M.J., Bundschuh, J., Panaullah, G., 2007. Arsenic in the environment: Biology and Chemistry. Sci. Total Environ. 379, 109–120. https://doi.org/10.1016/j.scitotenv.2007.02.037.

Bojko, O., Kabala, C., 2014. Loss-On-Ignition as an estimate of Total Organic Carbon in the mountain soils. Pol. J. Soil Sci. 47, 71–79. https://doi.org/10.1111/j.1365-2389.1964.tb00247.x.

Bridge, J.S., 2003. Rivers and Floodplains. Blackwell, Oxford, U.K., p. 491

Bundschuh, J., Farias, B., Martin, R., Storniolo, A., Bhattacharya, P., Cortes, J., Bonorino, G., Albouy, R., 2004. Groundwater arsenic in the Chaco-Pampean Plain, Argentina: Case study from Robles county, Santiago del Estero Province. Appl. Geochem. 19, 231–243. https://doi.org/10.1016/j.apgeochem.2003.09.009.

Campbell, J.R., Craw, D.D., Frew, R., Horton, T., Chamberlain, C.P., 2004. Geochemical signature of orogenic hydrothermal activity in an active tectonic intersection zone, Alpine Fault, New Zealand. Miner. Deposita 39, 437–451. https://doi.org/10.1007/s00126-004-0421-4.

Cao, W., Guo, H., Zhang, Y., Ma, R., Li, Y., Dong, Q., Li, Y., Zhao, R., 2018. Controls of paleochannels on groundwater arsenic distribution in shallow aquifers of alluvial plain in the Hetao Basin China. Sci. Total Environ. 613–614, 958–968. https://doi.org/10.1016/j.scitotenv.2017.09.182.

Chikkanna, A., Mehan, L., Sarath, P.K., Ghosh, D., 2019. Arsenic Exposures, poisoning, and threat to human health: Arsenic affecting human health. In: Papadopoulou, P., Marouli, C., Misseyanni, A. (Eds.), Environmental Exposures and Human Health Challenges. IGI Global, Hershey, PA, USA, pp. 86–105. https://doi.org/10.4018/978-1-5225-7635-8.ch004.

Das, D., Chatterjee, A., Samanta, G., Mandal, B., Chowdhury, T.R., Samanta, G., Chowdury, P.P., Chanda, C., Basu, G., Lodh, D., Nandi, S., Chakraborty, T., Mandal, S., Bhattacharya, S.M., Chakraborti, D., 1994. Arsenic contamination in groundwater in six districts of West Bengal, India: The biggest arsenic calamity in the world. Analyst 119, 168–170. https://doi.org/10.1039/AN994190168N.

Donselaar, M.E., Bhatt, A.G., Ghosh, A.K., 2017. On the relation between fluvio-deltaic flood basin geomorphology and the wide-spread occurrence of arsenic pollution in shallow aquifers. Sci. Total Environ. 574, 901–913. https://doi.org/10.1016/j.scitotenv.2016.09.074.

Donselaar, M.E., Overeem, I., 2008. Connectivity of fluvial point bar deposits: An example from the Miocene Huesca Fluvial Fan, Ebro Basin, Spain. AAPG Bullet. 92, 1109–1129. https://doi.org/10.1306/04180807079.

Freeze, R.A., Cherry, J.A., 1979. Groundwater. Englewood Cliffs, NJ, Prentice-Hall, p. 604.

Ghosh, D., Bhadury, P., 2018. Microbial Cycling of Arsenic in the Aquifers of Bengal Delta Plains (BDP). In: Adhya, T.K., Lal, B., Mohapatra, B., Paul, D., Das, S. (Eds.), Advances in Soil Microbiology: Recent Trends and Future Prospects, 1st ed,. Springer Singapore, pp. 91–108. https://doi.org/10.1007/978-981-10-6178-3_5.

Ghosh, D., Biswas, J.K., 2015. Biomonitoring macrophytes diversity and abundance for rating aquatic health of an oxbow lake ecosystem in Ganga River Basin. Am. J. Phytomed. Clin. Ther. 3, 602–621.

Ghosh, D., Kumar, S., Donselaar, M.E., Corroto, C., Ghosh, A.K., 2021. Organic Carbon transport model of abandoned river channels - A motif for floodplain geomorphology influencing biogeo-chemical swaying of arsenic. Sci. Total Environ. 762, 144400 https://doi.org/10.1016/j.scitotenv.2020.144400.

Ghosh, D., Routh, J., Bhadury, P., 2015a. Characterization and microbial utilization of dissolved lipid organic fraction in arsenic impacted aquifers (India). J. Hydrol. 527, 221–233. https://doi.org/10.1016/j.jhydrol.2015.04.051.

Ghosh, D., Routh, J., Bhadury, P., 2017. Sub-surface biogeochemical characteristics and its effect on arsenic cycling in the Holocene grey sand aquifers of the lower Bengal Basin. Front. Environ. Sc. 5, 82. https://doi.org/10.3389/fenvs.2017.00082.

Ghosh, D., Routh, J., Dario, M., Bhadury, P., 2015b. Elemental and biomarker characteristics in a Pleistocene aquifer vulnerable to arsenic contamination in the Bengal Delta Plain. India. Appl. Geochem. 61, 87–98. https://doi.org/10.1016/j.apgeochem.2015.05.007.

Göd, R., Zemann, J., 2000. Native arsenic - realgar mineralization in marbles from Saualpe, Carinthia, Austria. Mineralogy and Petrology 70, 37–53.

Guha Mazumder, D.N., Chakraborty, A.K., Ghose, A., Gupta, J.D., Chakraborty, D.P., Dey, S.B., Chattopadhyay, N., 1988. Chronic arsenic toxicity from drinking tubewell water in rural West Bengal. Bull. World Health Organ. 66, 499–506.

Guo, H.M., Yang, S.Z., Tang, X.H., Li, Y., Shen, Z.L., 2008. Groundwater geochemistry and its implications for arsenic mobilization in shallow aquifers of the Hetao basin. Inner Mongolia. Sci. Total Environ. 393, 131–144. https://doi.org/10.1016/j.scitotenv.2007.12.025.

Hartkamp-Bakker, C.A., Donselaar, M.E., 1993. Permeability patterns in point bar deposits: Tertiary Loranca Basin, central Spain. In: Flint, S.S., Bryant, I.D. (Eds.), The geological modelling of hydrocarbon reservoirs and outcrop analogues. Spec. Publ. Int. assoc. Sediment. 15, 157-168. https://doi.org/10.1002/9781444303957.ch9.

Harvey, C.F., Ashfaque, K.N., Yu, W., Badruzzaman, A.B.M., Ali, M.A., Oates, P.M., Michael, H.A., Neumann, R.B., Beckie, R., Islam, S., Ahmed, M.F., 2006. Groundwater dynamics and arsenic contamination in Bangladesh. Chem. Geol. 228, 112–136. https://doi.org/10.1016/j.chemgeo.2005.11.025.

Hillel, D., 1980. Applications of soil physics. Academic Press, New York, USA.

Holbrook, P., 2001. The primary controls over sediment compaction. In: Huffman, A.R., Bowers, G.L. (Eds.), Pressure regimes in sedimentary basins and their prediction. AAPG Mem. 76, 21–32. https://doi.org/10.1306/M76870.

Horton, T.W., Becker, J.A., Craw, D., Koons, P.O., Chamberlain, C.P., 2001. Hydrothermal arsenic enrichment in an active mountain belt: Southern Alps, New Zealand. Chem. Geol. 177, 323–339.

Huang, G., Sun, J., Ying, Z., Jing, J., Zhang, Y., Liu, J., 2011. Distribution of arsenic in sewage irrigation area of Pearl River Delta. China. J. of Earth Sci. 22, 396–410. https://doi.org/10.1007/s12583-011-0192-7.

Islam, F.S., Gault, A.G., Boothman, C., Polya, D.A., Chamok, J.M., Chatterjee, D., Lloyd, J.R., 2004. Role of metal-reducing bacteria in arsenic release from Bengal delta sediments. Nature 430, 68–71. https://doi.org/10.1038/nature02638.

Jakobsen, R., Kazmierczak, J., Sø, H.U., Postma, D., 2018. Spatial variability of groundwater arsenic concentration as controlled by hydrogeology: conceptual analysis using 2-D reactive transport modeling. Water Resources Research 54, 10254–10269. https://doi.org/10.1029/2018WR023685.

Kumar, S., Ghosh, D., Donselaar, M.E., Burgers, F., Ghosh, A.K., 2019. The arsenic-pollution problem: Volumetrics and mobilization processes of geogenic arsenic in Holocene clay-plug sediment. Abstract Book 34th IAS Meeting of Sedimentology.

Lawson, M., Polya, D.A., Boyce, A.J., Bryant, C., Mondal, D., ShantzBallentine, C.J., 2013. Pond-derived organic carbon driving changes in arsenic hazard found in Asian groundwaters. Environ. Sci. Technol. 47, 7085–7094. https://doi.org/10.1021/es400114q.

Linsley, R.K., Kohler, M.A., Paulhus, J.L.H., 1982. Hydrology for engineers, Third ed. McGraw-Hill, New York, USA.

McWhorter, D.B., Sunada, D.K., 1977. Groundwater hydrology and hydraulics. Water Resour. Publications, Fort Collins, CO. 290, 31 p.

Mondal, D., Rahman, M.M., Suman, S., Sharma, P., Siddique, A.B., Rahman, M.A., Bari, A.S.M.F., Kumar, R., Bose, N., Singh, S.K., Ghosh, A., Polya, D.A., 2021. Arsenic exposure from food exceeds that from drinking water in endemic area of Bihar. India. Sci. Total Environ. 754, 142082 https://doi.org/10.1016/j.scitotenv.2020.142082.

Mukherjee, A., Fryar, A.E., Scanlon, B., Bhattacharya, P., Bhattacharya, A., 2011. Elevated arsenic in deeper groundwater of the western Bengal basin, India: Extent and controls from regional to local scale. Appl. Geochem. 26, 600–613. https://doi.org/10.1016/j.apgeochem.2011.01.017.

Mukherjee, A., Gupta, S., Coomar, P., Fryar, A.E., Guillot, S., Verma, S., Bhattacharya, P., Bundschuh, J., Charlet, L., 2019. Plate tectonics influence on geogenic arsenic cycling: From primary sources to global groundwater enrichment. Sci. Total Environ. 683, 793–807. https://doi.org/10.1016/j.scitotenv.2019.04.255.

Mukherjee, A., Verma, S., Gupta, S., Henke, K.R., Bhattacharya, P., 2014. Influence of tectonics, sedimentation and aqueous flow cycles on the origin of global groundwater arsenic: paradigms from three continents. J. Hydrol. 518, 284–299. https://doi.org/10.1016/j.jhydrol.2013.10.044.

Nichols, G., 2009. Sedimentology and stratigraphy, second ed. Wiley-Blackwell, New Jersey, USA, p. 432.

Nickson, R., McArthur, J., Burgess, W., Ahmed, K.M., Ravenscroft, P., Rahman, M., 1998. Arsenic poisoning of Bangladesh groundwater. Nature 395, 338. https://doi.org/10.1038/26387.

Postma, D., Larsen, F., Thai, N.T., Trang, P.T.K., Jakobsen, R., Nhan, P.Q., Long, T.V., Pham, H.V., Murray, A.S., 2012. Groundwater arsenic concentration in Vietnam controlled by sediment age. Nat. Geosci. 5, 656–661. https://doi.org/10.1038/NGEO1540.

Postma, D., Mai, N.T.H., Lan, V.M., Trang, P.T.K., Sø, H.U., Nhan, P.Q., Larsen, F., Viet, P.H., Jakobsen, R., 2016. Fate of arsenic during Red River water infiltration into aquifers beneath Hanoi Vietnam. Environ. Sci. Technol. 51, 838–845. https://doi.org/10.1021/acs.est.6b05065.

Quino Lima, I., Eduardo Ramos Ramos, O., Ormachea Muñoz, M., Isabel Chambi Tapia, M., Quintanilla Aguirre, J., Ahmad, A., Prakash Maity, J., Tahmidul Islam, Md., Bhattacharya, P., 2021. Geochemical mechanisms of natural arsenic mobility in the hydrogeologic system of Lower Katari Basin, Bolivian Altiplano. J. Hydrol. 594, 125778. https://doi.org/10.1016/j.jhydrol.2020.125778.

Ramos, O.E., Rötting, T.S., French, M., Sracek, O., Bundschuh, J., Quintanilla, J., Bhattacharya, P., 2014. Geochemical processes controlling mobilization of arsenic and trace elements in shallow aquifers and surface waters in the Antequera and Poopó mining regions, Bolivian Altiplano. J. Hydrol. 518, 421–433. https://doi.org/10.1016/j.jhydrol.2014.08.019.

Ravenscroft, P., Brammer, H., Richards, K., 2009. Arsenic in Asia. In: Ravenscroft, P., Brammer, H., Richards, K. (Eds.), Arsenic Contamination: A Global Synthesis. Wiley-Blackwell, Oxford, UK, pp. 318–386.

Richards, L.A., Magnone, D., Boyce, A.J., Casanueva-Marenco, M.J., van Dongen, B.E., Ballentine, C.J., Polya, D.A., 2018. Delineating sources of groundwater recharge in an arsenic-affected Holocene aquifer in Cambodia using stable isotope-based mixing models. J. Hydrol. 557, 321–334. https://doi.org/10.1016/j.jhydrol.2017.12.012.

Saha, K.C., 1984. Melanokeratosis from arsenical contamination of tubewell water. Indian. J. Dermatol. 29, 37–46.

Saha, K.C., 2003. Diagnosis of Arsenicosis. J. Environ. Sci. Health Part A 38, 255–272. https://doi.org/10.1081/ESE-120016893.

Saha, D., 2009. Arsenic groundwater contamination in parts of middle Ganga plain. Bihar. Curr. Sci. 97, 753–755.

Sahu, S., Saha, D., 2015. Role of shallow alluvial stratigraphy and Holocene geomorphology on groundwater arsenic contamination in the Middle Ganga Plain India. Environ. Earth Sci. 73, 3523–3536. https://doi.org/10.1007/s12665-014-3637-3.

Seddique, A.A., Masuda, H., Mitamura, M., Shinoda, K., Yamanaka, T., Itai, T., Maruoka, T., Uesugi, K., Ahmed, K.M., Biswas, D.K., 2008. Arsenic release from biotite into a Holocene groundwater aquifer in Bangladesh. Appl. Geochem. 23, 2236–2248. https://doi.org/10.1016/j.apgeochem.2008.03.007.

Shah, B.A., 2008. Role of Quaternary stratigraphy on arsenic-contaminated groundwater from parts of Middle Ganga Plain, UP-Bihar. India. Environ. Geol. 53, 1553–1561. https://doi.org/10.1007/s00254-007-0766-y.

Shah, B.A., 2010. Arsenic-contaminated groundwater in Holocene sediments from parts of Middle Ganga Plain, Uttar Pradesh. India. Curr. Sci. 98, 1359–1365.

Shah, B.A., 2017. Arsenic contamination in groundwater affecting Holocene aquifers of India: A review. In: Kurusi, F., Ramanathan, A., Kazmi, A.A., Kumar, M. (Eds.), Trends in Asian Water Environmental Science and Technology. Springer Int. Publ., Cham, Switzerland, Capital Publ. Co., New Delhi, India, pp. 157–167. https://doi.org/10.1007/978-3-319-39259-2.

Singer, A., Müller, G., 1983. Diagenesis in argillaceous sediments. In: Larsen, G., Chillingar, G.V. (Eds.), Diagenesis in Sediments and Sedimentary Rocks 2. Elsevier Amsterdam, pp. 115–212.

SIS, 1993. Vattenundersökningar – Bestämning av metaller med atom absorptions spektrometri i flamma – Allmänna principer och regler (Translated title: Water analysis – Determination of metals by atomic absorption spectrometry, atomization inflame – General principles and guidelines). Swedish Standard Method SS 02 81 50, 6 p.

Smedley, P.L., Kinniburgh, D.G., 2002. A review of the source, behaviour and distribution of arsenic in natural waters. Appl. Geochem. 17, 517–568. https://doi.org/10.1016/S0883-2927(02)00018-5.

Smith, A.H., Lingas, E.O., Rahman, M., 2000. Contamination of drinking-water by arsenic in Bangladesh: a public health emergency. Bull. WHO 78, 1093–1103.

Stone, W.N., Siever, R., 1996. Quantifying compaction, pressure solution and quartz cementation in moderately- and deeply-buried quartzose sandstones from the Greater Green River Basin, Wyoming. In: Crossey, L.J., Loucks, R., Totten, M.W. (Eds.), Siliciclastic Diagenesis and Fluid Flow: Concepts and applications. SEPM Special Publication, pp. 129–150, 10.2110/pec.96.55.0129.

Stopelli, E., Duyen, V.T., Mai, T.T., Trang, P.T.K., Viet, P.H., Lightfoot, A., Kipfer, R., Schneider, M., Eiche, E., Kontny, A., Neumann, T., Glodowska, M., Patzner, M., Kappler, A., Kleindienst, S., Rathi, B., Cirpka, O., Bostick, B., Prommer, H., Winkel, L. H.E., Berg, M., 2020. Spatial and temporal evolution of groundwater arsenic contamination in the Red River delta, Vietnam: Interplay of mobilisation and retardation processes. Sci. Total Environ. 717, 137143 https://doi.org/10.1016/j.scitotenv.2020.137143.

Tapia, J., Murray, J., Ormachea, M., Tirado, N., Nordstrom, D.K., 2019. Origin, distribution, and geochemistry of arsenic in the Altiplano-Puna plateau of Argentina, Bolivia, Chile, and Perú. Sci. Total Environ. 678, 309–325. https://doi.org/10.1016/j.scitotenv.2019.04.084.

Trung, D.T., Nhan, N.T., Don, T.V., Hung, N.K., Kazmierczak, J., Nhan, P.Q., 2020. The controlling of paleo-riverbed migration on Arsenic mobilization in groundwater in the Red River Delta Vietnam. Vietnam J. Earth Sci. 42, 161–175. https://doi.org/10.15625/0866-7187/42/2/14998.

von Brömssen, M., Jakariya, M., Bhattacharya, P., Ahmed, K.M., Hasan, M.A., Sracek, O., Jonsson, L., Lundell, L., Jacks, G., 2007. Targeting low-arsenic aquifers in Matlab Upazila Southeastern Bangladesh. Sci. Total Environ. 379, 121–132. https://doi.org/10.1016/j.scitotenv.2006.06.028.

von Brömssen, M., Larsson, S.H., Bhattacharya, P., Hasan, M.A., Ahmed, K.M., Jakariya, M., Sikder, M.A., Sracek, O., Bivén, A., Doušová, B., Patriarca, C., Thunvik, R., Jacks, G., 2008. Geochemical characterisation of shallow aquifer sediments of Matlab Upazila, Southeastern Bangladesh — Implications for targeting low-As aquifers. J. Contam. Hydrol. 99, 137–149. https://doi.org/10.1016/j.jconhyd.2008.05.005.

Wallis, I., Prommer, H., Berg, M., Siade, A.J., Sun, J., Kipfer, R., 2020. The river–groundwater interface as a hotspot for arsenic release. Nature Geosci. 13, 288–295. https://doi.org/10.1038/s41561-020-0557-6.

Weinman, B., Goodbred Jr., S.L., Zheng, Y., Aziz, Z., Steckler, M., van Geen, A., Singhvi, A.K., Nagar, Y.C., 2008. Contributions of floodplain stratigraphy and

evolution to the spatial patterns of groundwater arsenic in Araihazar Bangladesh. Geol. Soc. Am. Bull. 120, 1567–1580. https://doi.org/10.1130/B26209.1.

World Health Organization (WHO), 1993. Guidelines for Drinking-Water Quality. 2nd ed. Recommendations 1, 41–42.

World Health Organization (WHO), 2011. Guidelines for Drinking-Water Quality. 4th ed. Geneva, 541 p.

Yu, C., Loureiro, C., Cheng, J.J., Jones, L.G., Wang, Y.Y., Chia, Y.P., Faillace, E., 1993. Data Collection Handbook to Support Modeling Impacts of Radioactive Material In Soil. ANL/EAIS-8, Argonne National Laboratory, Argonne, IL, 163 p. https://doi.org/10.2172/10162250.

Zheng, Y., van Geen, A., Stute, M., Dhar, R., Mo, Z., Cheng, Z., Horneman, A., Gavrieli, I., Simpson, H.J., Versteeg, R., Steckler, M., Goodbred, S., Ahmed, K.M., Shanewaz, M., Shamsudduha, M., 2005. Contrast in groundwater arsenic in shallow Holocene and older deep aquifers: A case study in two villages of Araihazar, Bangladesh. Geochimica et Cosmochimica Acta 69, 5203–5218. https://doi.org/10.1016/j.gca.2005.06.001.